Seismic Soil Structure Interaction Response of Midrise Concrete Structures on Silty Sandy Soil

Sahar Ismail [1)]***, Fouad Kaddah*** [2)] ***and Wassim Raphael*** [3)]

[1)] PhD Researcher, Civil Engineering Department, Saint Joseph University of Beirut, Beirut 17-5208, Lebanon. E-Mail: sahar.ismail@net.usj.edu.lb
[2)] Professor, Civil Engineering Department, Saint Joseph University of Beirut, Beirut 17-5208, Lebanon. E-Mail: fouad.kaddah@usj.edu.lb
[3)] Professor, Civil Engineering Department, Saint Joseph University of Beirut, Beirut 17-5208, Lebanon. E-Mail: wassim.raphael@usj.edu.lb

ABSTRACT

The seismic response of midrise frame structures rested on soft soils is susceptible to the dynamic interaction between structure, foundation and soil, called soil structure interaction (*SSI*). While seismic codes provide design acceleration charts based on 1D free-field response analysis, research into *SSI* is limited compared to other structural and geotechnical topics and does not consider all parameters covering the interaction between structure, foundation and soil. In this study, a series of 3D finite element analyses were conducted using Abaqus to investigate the effects of midrise structures' number of stories as well as raft and column dimensions while considering *SSI* effects divided between inertial and kinematic. In the analyses, the frame structure was assumed to be rested on a raft foundation and silty sandy soil block and the model was hit at bottom by El-Centro (1940) and Northridge (1994) earthquakes. Moreover, the response of the structure was studied for (1) fixed-based and (2) flexible-based structures. Results, presented in terms of storey lateral displacement, inter-storey drifts, shear force, foundation rocking and response spectrum, indicate that *SSI* effects divide midrise structures into 2 categories: (1) $5 \leq N < 10$ and (2) $10 \leq N \leq 15$. In fact, *SSI* was beneficial for the first category, while it was detrimental to the second. Moreover, different behaviours were obtained for different column sizes when varying raft sizes and thicknesses. Thus, engineers should carefully optimize their design between these different studied parameters, where an increase in column size with raft dimension caused a decrease in foundation rocking angle, while structural stability and failure depended highly on column size.

KEYWORDS: Abaqus, Soil structure interaction, Silty sandy soil, Inelastic seismic response, Fully nonlinear method, Midrise moment-resisting frame.

Notation List

SSI=soil structure interaction, *FF*=free field, *N*=number of stories, *c*=soil apparent cohesion value (kPa), γ_d=dry unit weight (kN/m^3), Φ=internal friction angle (°), Ψ = dilation angle (°), E = Young modulus (MPa), G = shear modulus (MPa), f'_c = concrete compressive strength (MPa), e =void ratio, v=Poisson's ratio, PI = plasticity index(%), γ_c: cyclic shear strain, A=acceleration(g), PGA=peak ground acceleration (g), S_a=spectral acceleration (g), ζ=damping ratio (%), d_i=deflections at i level (mm), h= storey height (m), α=mass damping factor, β=stiffness damping factor, f_i =mode frequency (Hz), $[M]$,$[C]$ and $[K]$= mass, damping and stiffness matrices of the structure, $\{u\}$, $\{\dot{u}\}$, $\{\ddot{u}\}$= nodal lateral displacements, velocities and

Received on 26/1/2020.
Accepted for Publication on 17/2/2020.

accelerations with respect to the underlying soil foundation, $\ddot{u}_g$= earthquake acceleration at the base of the model, $\{F_v\}$= force vector corresponding to soil quiet boundaries, B= width of structure (m), R= width of raft (m), e= raft thickness (m), C=column size, V = base shear (kN), δ=lateral deflection (m), $h_j\phi_o$ = lateral displacement due to rocking component (m), U_j:= displacement due to distortion component (m), U_j^{tot}=horizontal displacement at level j of the structure (m), U_1^{tot}=horizontal displacement at the ground level (m), U_g= horizontal ground motion at the surface caused by the passage of the earthquake, U_f = relative deformation of the structure (m), U_o = horizontal deformation (m), Φ_o= rocking angle of rigid foundation.

INTRODUCTION

The seismic response of a structure is affected by the response of the soil medium, where the structure and the foundation are founded. Midrise structures have been built in areas prone to earthquakes for several decades. Thus, researchers have been studying the effects of earthquakes on soils and structures since early 1960s. Since then, several seismic events occurred and expanded researchers' knowledge on this topic, such as the 1994 M_w=6.7 Northridge and 1995 M_w=7.5 Kobe earthquakes. Recently, two strong earthquakes hit urbanized neighbourhoods and left important damages on lives and structures: Ridgecrest (2019) M_w=7.1 and Albania (2019) M_w=6.4. Veletsos and Meek (1974), Wolf (1985), Luco et al. (1988), Gazetas and Mylokanis (1998), Stewart et al. (1999), ATC (2012), Farghali and Ahmed (2013) and Tabatabeifar et al. (2014b) are among many other researchers who showed the importance of considering *SSI* effects in designing structures against earthquake loads to ensure safe designs. *SSI* refers to the dynamic interaction between the structure and the underlying soil or rock. Seismic *SSI* has been beneficial to structures founded on soft soils; so most seismic codes neglect its effect as a means to improve the factor of safety. Nevertheless, Stewart et al. (1999), Mylonakis and Gazetas (2000) and Shehata et al. (2015) investigated the conservatism and gaps in seismic codes and showed that *SSI* can be detrimental in soft soils.

The influence of *SSI* on structures supported by raft and pile foundations was studied in the literature using analytical, experimental and numerical solutions using the finite element software: Abaqus, ETABs, SAP2000, Ansys,… etc. and the finite difference software: Flac. Fatahi and Tabatabaiefar (2014) found that the equivalent linear method underestimates the inelastic response of midrise buildings resting on soft soils compared to fully nonlinear method leading to underestimating the structure performance level. Han (2002), Farghali and Ahmed (2013), Tabatabeifar et al. (2014b), Shehata et al. (2015), Nadar et al. (2015) and Jayalekshmi and Chinmayi (2016) found that flexible base cases, lateral deflection gets amplified compared to that of fixed base cases, while base shear gets reduced. Shehata et al. (2015) and Nadar et al. (2015) found that *SSI* increases the displacement of the building's storey that gets mostly affected at the lower stories. Torabi and Rayhani (2014) found that rigid slender structures are highly prone to *SSI* effects manifested by the changes in the structure's natural frequency, shear forces and foundation rocking.

The effect of dampers on seismic design of structures was investigated by several researchers. Recently, Armouni (2010, 2011) obtained that structures rested on rock sites exhibited less amount of seismic demand and sensitivity compared to other soil sites. Nevertheless, he recommends designing short structures with dampers to obtain higher levels of safety. Shatnawi and al-Qaryouni (2018) found that viscoelastic dampers amplify seismic force reduction, overall ductility and strength factors that tend to increase with the structure's number of stories. Bayat et al. (2018) showed that multiple tuned mass dampers are more effective than single tuned mass dampers, while Djedoui et al. (2018) found that semi-active tunes mass dampers with variable damping were better than traditional tunes mass dampers with constant

dampers in reducing base-isolated building response.

Regarding the effect of foundation type, Shehata et al. (2015) proved that storey shear response depends on foundation and soil type, while Kumar et al. (2016) found that the response of a foundation depends on the input motion. On the other hand, Hokmabadi and Fatahi (2016) showed that earthquake motion characteristics are affected by the structure as well as by the foundation type. Yingcai (2002), Hokmabadi et al. (2012, 2014) and Hokmabadi and Fatahi (2016) found that shallow foundation causes higher deformation, but lower base shear and foundation rocking compared to pile foundation. Moreover, Nguyen et al. (2016) obtained that structures with smaller shallow foundations survive stronger earthquakes. Finally, Turan et al. (2013) showed that the increase in foundation embedment depth increases flexible structure's frequency that approaches fixed-base structure's frequency.

Therefore, many researchers discussed the significance and importance of *SSI* on structural response and design. These structures were rested on either cohesionless or cohesive soil. Nevertheless, research into *SSI* is limited compared to other structural and geotechnical topics and does not tackle all parameters covering the interaction between the structure, foundation and soil. Hence, 3D time history finite element model analysis of midrise storey concrete frame structures supported by raft foundation and founded on a silty sandy soil block was performed using Abaqus under the influence of two strong ground motions: El-Centro (1940) and Northridge (1994) earthquakes. The effects of varying midrise structures' number of stories as well as raft size and thickness for different column sizes were investigated in this paper by comparing the lateral displacement, inter-storey drift, shear force, foundation rocking and response spectrum results of flexible to fixed-base structures. The main goal of this study was to check the contribution of the studied parameters on inertial and kinematic interactions to aid engineers obtain economical and safe seismic designs.

NUMERICAL MODELLING AND ANALYSIS OF THE MODEL

Problem Definition

The finite element software Abaqus 2017 was used to study the seismic behaviour of midrise concrete frame structures by varying structures' number of stories as well as raft dimensions: sizes and thicknesses, for two different column sizes under El-Centro (1940) M_w=6.9, PGA=0.318g far-field and Northridge (1994) M_w=6.7, PGA=0.843g near-field earthquakes. Both earthquakes are rock outcrop motions (Fig. 1); so all models performed in this paper were hit at the bottom by these strong ground motions, as shown in Fig. 2. Two kinds of 3D nonlinear time history models were simulated: "S-models" representing fixed based structures and "S-F-models" representing flexible base structures consisting of a frame structure founded on a raft foundation and both rested on a dense silty sandy soil block. The characteristics of all performed simulations along with their nomenclatures are detailed in Tables 1, 2 and 3. The 3D models were simulated using the direct method of analysis: the entire structure-foundation-soil was modelled at the same time and the input earthquake load was applied at the base of the model. Thus, the dynamic equation of motion of the soil-foundation-structure system can be written as:

$$[M]\{\ddot{u}\} + [C]\{\dot{u}\} + [K]\{u\} = -[M]\{m\}\ddot{u}_g + \{F_v\}.$$

When plasticity is included, $[K]$ is the tangential matrix, $\ddot{u}_g$ is the earthquake acceleration at the base of the model and $\{m\} = [1,0,0,1,0,0,\ldots,0]^T$, since only horizontal acceleration was considered in this article.

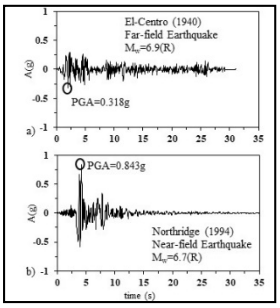

Figure (1): Acceleration with respect to time of a) El-Centro (1940) and b) Northridge (1994) earthquakes

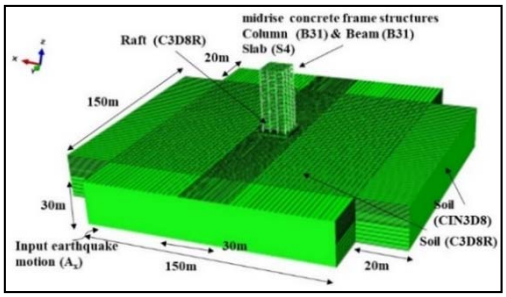

Figure (2): Geometry and model mesh distribution

Table 1. Finite element model characteristics

Number of Bays	Storey Height	Bay Width (m)	E_c (GPa)
3	3	5	14
Column Size (m)		**Slab**	**Beam Size (m)**
0.5 X 0.5 m, 0.5 X 1 m		5 X 5 X 0.25	0.5 X 0.5 m

Table 2. Structures' mass and damping factors

C (m)	0.5 X 1	0.5 X 0.5				
	S15	S15	S12	S10	S7	S5
α	0.25	0.22	0.29	0.32	0.5	0.52
β	0.007	0.008	0.007	0.006	0.004	0.003

Model Characteristics

The beams and columns were built in the finite element models using 2-node linear beam elements B31 with 9400 elements. In additions, the slab was built using 4-node doubly curved shell with 100 elements. 2.5 kN/m^2 uniformly distributed dead and live loads were applied to the structures' floors. All frames were supported on a solid raft foundation and modelled using eight-node linear brick, reduced-integration, hourglass control continuum solid elements C3D8R with 4800 elements. The frame and the structure were rested on a soil medium modelled using eight node linear brick, reduced-integration, hourglass control continuum solid elements C3D8R with 96500 elements. To account for the absorbed energy from the unbounded soil domain in the horizontal directions, far field soil was represented by 8-node linear one-way infinite brick elements CIN3D8. These elements have defined orientation: the first 4 nodes (nodes 1-4) should be connected to the defined soil element C3D8R, while the other 4 nodes (nodes 5-8) should be oriented in the outward direction. In addition, the bottom soil boundary was modelled as a rigid boundary to simulate bedrock.

Table 3. Finite element model configuration

	Reference name	N	Raft dimension length X width X thickness (m)	C (m)
Number of stories	**S15**	15	-	0.5 X 0.5
	S15-e-1.5m	15	20 X 20 X 1.5	0.5 X 0.5
	S12	12	-	0.5 X 0.5
	S12-e-1.2m	12	20 X 20 X 1.2	0.5 X 0.5
	S10	10	-	0.5 X 0.5
	S10-e-1m	10	20 X 20 X 1	0.5 X 0.5
	S7	7	-	0.5 X 0.5
	S7-e-0.7m	7	20 X 20 X 0.7	0.5 X 0.5
	S5	5	-	0.5 X 0.5
	S5-e-0.5m	5	20 X 20 X 0.5	0.5 X 0.5

Raft and Column Sizes	**S15-1.3B**	15	20 X 20 X 1.5	0.5 X 0.5
	S15-1.5B	15	22.5X 22.5 X 1.5	0.5 X 0.5
	S15-2B	15	30 X 30 X 1.5	0.5 X 0.5
	S15-1.3B-C-0.5-1m	15	20 X 20 X 1.5	0.5 X 1
	S15-1.5B-C-0.5-1m	15	22.5X 22.5 X 1.5	0.5 X 1
	S15-2B-C-0.5-1m	15	30 X 30 X 1.5	0.5 X1
Raft Thickness and Column Sizes	**S15**	15	-	0.5 X 0.5
	S15-e-2m	15	20 X 20 X 1.5	0.5 X 0.5
	S15-e-1.5m	15	20 X 20 X 1.5	0.5 X 0.5
	S15-e-1m	15	20 X 20 X 1.5	0.5 X 0.5
	S15- C-0.5-1m	15	-	0.5 X 1
	S15-e-2m-C-0.5-1m	15	20 X 20 X 1.5	0.5 X 1
	S15-e-1.5m-C-0.5-1m	15	20 X 20 X 1.5	0.5 X 1
	S15-e-1m- C-0.5-1m	15	20 X 20 X 1.5	0.5 X 1

To simulate structure-raft-soil interface, beams and floor slabs were tied in the frame structure, where a special tie procedure was performed between the columns and the raft, while the raft bottom surface and soil top surface were tied in the numerical models. Moreover, embedded columns were inserted in the raft in S-F-models. Using a linear perturbation procedure and Lancoz method, eigen values and thus natural frequencies as well as models' mode shapes were calculated *via* Abaqus. Reinforced concrete having 2400 kg/m^3 density and 0.2 Poisson's ratio was used throughout the analyses. Elastic-perfectly plastic material was used to model the inelastic behaviour of structural elements while considering 5% structural (ζ) Rayleigh damping. Therefore, based on first and second mode frequencies (f_i and f_j in rad/s) (Table 2), α and β were calculated as follows (Chopra, 2011):

$$\zeta = \frac{1}{2f_n}\alpha + \frac{f_n}{2}\beta, \alpha = 2\zeta_i \frac{f_i f_j}{f_i + f_j}, \beta = 2\zeta_i \frac{1}{f_i + f_j}.$$

The frame structures were rested on a silty sandy soil the properties of which are detailed in Table 4. To calculate the wave propagation in the soil medium subjected to a seismic excitation, the equivalent linear method was used (Seed and Idriss, 1969; Vucetic and Dobry, 1991; Park and Hashash, 2003). In this method, a linear analysis with preliminary assumed values for shear modulus and damping ratio in different regions of the model was performed. Then, the maximum cyclic shear strain of all soil elements was recorded; this strain was then implemented in the backbone curves given by Vucetic and Dobry (1991) that relate the shear modulus and damping ratio to the cyclic shear strain for different soil plasticity indices for cohesive soils. The new values obtained from these curves were then used in the numerical model. This stage was repeated until no further change in the soil properties and structural behaviour was obtained and thus, the obtained values were assumed to reflect the closest prediction of real soil behaviour, noting that the values of soil damping, and shear modulus obtained are unique for every earthquake-soil medium. This is because every earthquake produces different shear strain levels in the soil medium. Therefore, using first and second mode soil block frequencies obtained from Abaqus and Rayleigh damping, α and β were calculated for each earthquake, as summarized in Table 4.

Table 4. Soil properties

E (MPa)	v	γ_d (kN/m^3)	e	ϕ (°)	Ψ (°)	c (kPa)
20	0.3	18.98	0.4	35	10	50
	γ_c (%)	G/G_{max}	ζ (%)	α	β	PI (%)
El-Centro (1940)	1.72	0.085	20	0.63	0.066	15
Northridge (1994)	1.82	0.0769	21	0.65	0.068	15

Every time history model took around 60 hours to be completed using fast computational facilities at Saint Joseph University of Beirut, noting that to optimize the accuracy of the results with simulation computational speed, parametric studies were performed to obtain proper element mesh sizes and soil boundary limits. Thus, a mesh sensitivity analysis was performed along with varying soil boundary limits in both horizontal directions in order to obtain insignificant wave effects (not shown due to page size limits). The results showed that the soil boundary limit in both horizontal directions should be taken equal to 10B or 7.5R (=150 m) with B being the width of the structure and R the width of the raft foundation and increasing the soil limit from 4R to 9R (5.5B to 12B) led to 30 % difference in lateral defection results. Thus, the obtained results proved that soil boundary limits should be taken greater than the recommended values given by Ghosh and Wilson (1969) and Rayhani and El Naggar (2008).

NUMERICAL RESULTS AND ANALYSIS

The resisting of frame structures to mitigate seismic load was evaluated using three-dimensional finite element modelling of the simulated conditions hit at the bottom by El-Centro (1940) and Northridge (1994) earthquakes. Storey lateral deflection, inter-storey drift, shear force, foundation rocking and response spectrum were reported and calculated for all modelled scenarios. Stories lateral deflection and thus inter-stories drifts were calculated for two cases: (1) at max top: when the maximum lateral deflection occurred at top of the structure and (2) at abs max: when the maximum lateral deflection occurred at each storey level regardless the time it occurred (after Homabadi et al., 2012b). Note that the lateral deflection at each storey was measured relative to the lateral deflection at the base of the structure. Inter-storey drift was calculated as the difference between the deflections of two successive stories when the building is subjected to an earthquake load, normalized by the storey height: $drift = (d_{i+1} - d_i)/h$, where d_{i+1} and d_i are the deflections at $i+1$ and i levels, respectively. Inter-storey drift, a performance damage parameter, expresses the level of damage produced by an earthquake on a structure based on safety and risk assessment. Thus, performance levels are classified into categories depending on the inter-storey drift value (BSSC 1997, 2009). Most design codes limit inter-storey drift values to guarantee meeting deformation-base criteria. For example, the Australian Earthquake Code (AS1170.4 2007) limits the maximum allowable storey drift to 1.5%, while ASCE7-10 (2010) limits the allowable storey drift due to the structure's type and risk category.

The maximum lateral deflections and thus, inter-storey drifts experienced by a structure during an earthquake are in fact affected by the amount of structural rocking. Rocking occurs when the inertial forces in a structure cause compression on one side of the foundation and tension on the other side. Kramer (1996) divided the relative lateral structural displacement under the influence of soil structure interaction into two components: rocking and distortion. In other words, Kramer (1996) related the changes in

storey displacements to the changes in these components. Thus, foundation rocking was calculated as the difference in uplift raft displacement along earthquake loading divided by the raft width and expressed in degrees. In addition, shear forces produced by every column at every storey were summed up during the time history analysis and then the absolute maximum shear force at that level was recorded. Then, shear force plots were produced along with response spectrum curves to reflect the amount of energy that the structure absorbs during the strong motion. Thus, pseudo-acceleration response spectrum (S_a) plots were created for horizontal accelerations produced at the base of the modelled structures. The variation of single degree of freedom (SDF) pseudo-acceleration with different natural periods at 5% damping was generated using FORTRAN code. Finally, Fourier transformation of strong ground motion acceleration of the input earthquake, at the top of the soil profile (*FF*) and at the base of the structure-foundation model at 5% damping, were produced using MATLAB. These plots express the frequency content of a motion: a narrow curve implies a dominant frequency (smooth time history), while a broad curve implies variation of frequencies (irregular time history). Note that response spectrum plots are used in structure dynamic designs to calculate the necessary base shear forces as a function of soil-foundation-structure natural frequency.

The soil material adopted in our analyses is a granular soil with silt the presence of which imparts a degree of apparent cohesion. Such material is typical of Lebanese mountainous areas. A comprehensive parametric study was conducted to investigate the effects of structure's number of stories, raft thickness, raft size and column size as detailed in Table 3. Thus, the parametric studies were structured around a baseline case, from which all various parameters were varied individually in a controlled manner and the response of the structure was documented along with inertial and kinematic interaction responses. The baseline case consisted of the following: (1) number of Stories, N=15 (S15 structure consisting of 45 m high X 15 m wide), (2) 3 X 5 m bays (in X and Y directions), (3) column size: C=0.5X0.5 m, (4) raft foundation width 1.3B=20 m and thickness e=1.5 m and (5) soil block: 150 m X 150 m wide and 30 m height.

Effect of Number of Stories

Buildings can be divided into low-, medium- and high-rise buildings depending on the number of stories (N): if $N \leq 5$: low-rise buildings, if $5 \leq N \leq 15$: medium-rise buildings and if $N \geq 15$: high-rise buildings. The range of number of stories within medium-rise buildings category suggests the need to consider its effect in the evaluation of seismic structure's response while considering *SSI* effects. In order to address and quantify the contribution of structure's number of stories to inertial and kinematic effects, structures' storey number was varied between 5, 7, 10, 12 and 15 around the baseline case.

Storey Lateral Deflection and Inter-storey Drifts

The lateral deflection curves in Fig. 3 and Fig. 4 clearly demonstrate the significant contribution of number of stories to stories' lateral deflection and inter-storey drifts. The results showed that midrise structures having $5 \leq N \leq 15$ are divided into two categories: (1) $5 \leq N < 10$ and (2) $10 \leq N \leq 15$. The seismic behaviour of frame structures founded on silty sandy soil of the second category; i.e., when N is greater than 10, is like that of those founded on soft soils where *SSI* increases structure's lateral displacement. This is in parallel with others (Farghali and Ahmed, 2013; Shehata et al., 2015; Nadar et al., 2015). Thus, the lateral deflections of frame structure behaviour of the first category; i.e., when $5 \leq N < 10$, are greater in fixed than in flexible cases. As shown in Fig. 3 and Fig. 4, at max top which presents a more critical scenario than at abs max, the ratio of flexible to fixed cases lateral deflection at top of the structure (at structure's final storey) of S15, S12, S10, S7 and S5 is equal to 1.90, 1.40, 1.29, 0.76 and 0.54 under the influence of El-Centro (1940) and equal to 1.61, 1.67, 1.68, 0.46 and 0.91 under Northridge (1994). This ratio is related to the amount of energy that the raft

and soil absorb caused by the changes in dynamic characteristics of the structure-soil-foundation system under the seismic excitation.

As shown in Table 5, the results clearly demonstrate the attenuation of the wave when it reached *FF* under both earthquakes. The maximum input earthquake acceleration was attenuated from 3.13 m/s^2 and 8.24 m/s^2 to 0.783 m/s^2 and 3.13 m/s^2 at FF under El-Centro (1940) and Northridge (1994) earthquakes, respectively. Therefore, the results found in this paper were not in accordance with studies conducted by other researchers who used clayey soil, where the wave is expected to amplify when reaching soil surface (Farghaly and Ahmed, 2013; Hokmabadi et al., 2012; Tabatabaiefar et al., 2014), etc). Nevertheless, like Rayhani and El Naggar (2008), the wave got amplified below the structure compared to *FF* motion showing the effect of *SSI*. The maximum acceleration got amplified from 0.783 m/s^2 and 3.13 m/s^2 at *FF* to an average value of 1.33 m/s^2 and 5.36 m/s^2 at the base of the flexible frame structures under El-Centro (1940) and Northridge (1994) earthquakes, respectively. Thus, the maximum wave acceleration value significantly increased from S5 to S15 cases, while it decreased from fixed to flexible cases under all scenarios, as detailed in Table 5. Therefore, even though accelerations were amplified from the base to the top of fixed and flexible structures and flexible structures exhibited lower acceleration values than fixed based structures at the top of structures in all simulated cases, the behaviour of the first frame structures' category was the opposite compared to that of the second category. Note that even though a shear wall-based structure design should be used under Northridge (1994) earthquake, the authors used Northridge (1994) excitation in this paper on a moment frame building to compare with the behaviour of the frame structure under El-Centro (1940) excitation.

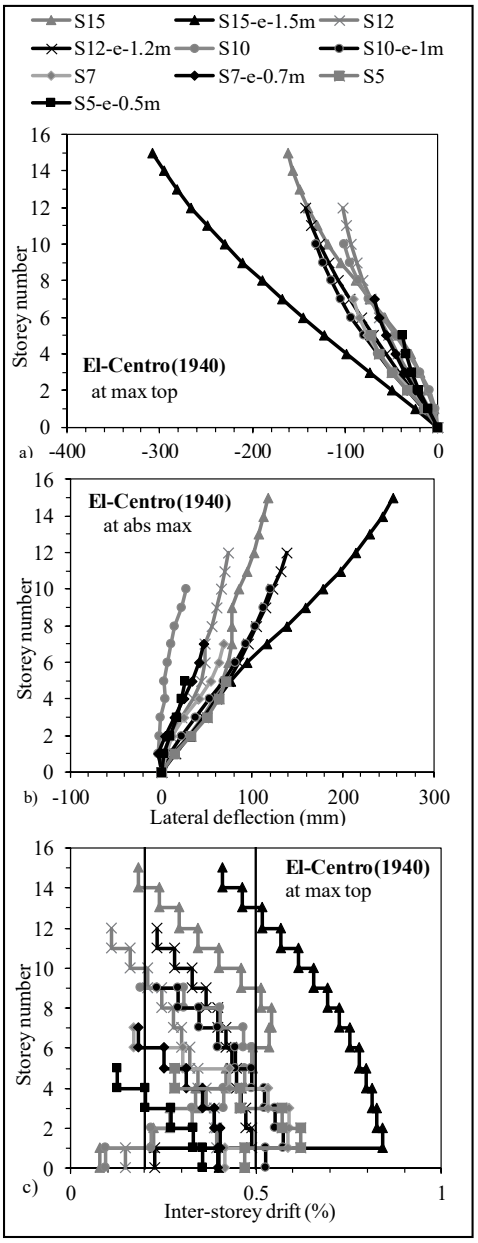

Figure (3): Variation of lateral deflection a) at max top, b) at abs max and c) variation of inter-storey drift at max top with storey number under El-Centro (1940) earthquake: effect of structure's number of stories

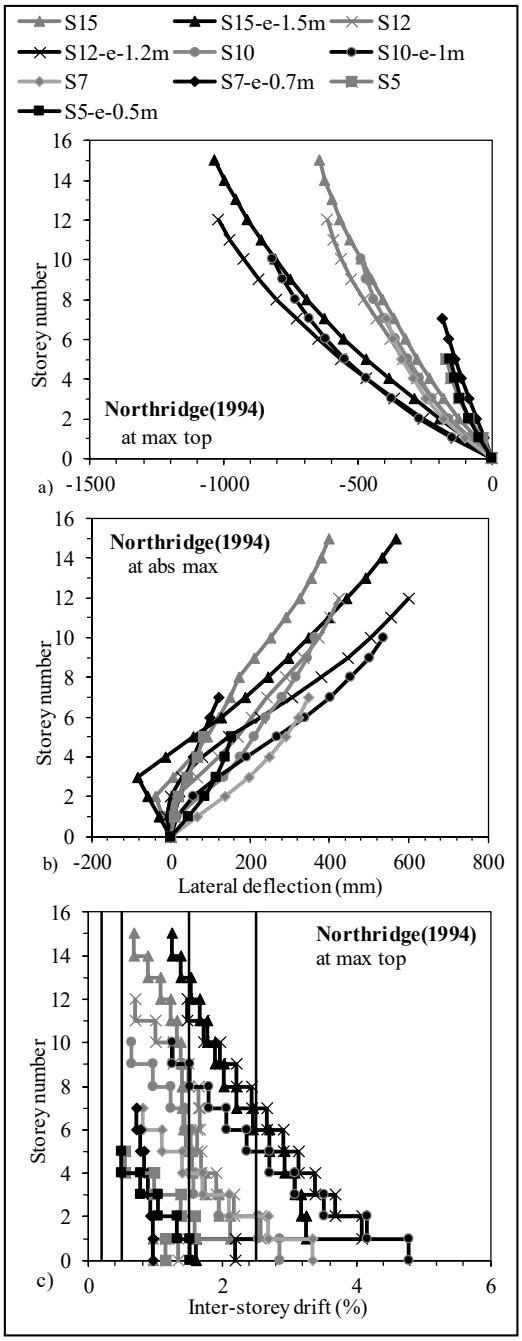

Figure (4): Variation of lateral deflection a) at max top, b) at abs max and c) variation of inter-storey drift at max top with storey number under Northridge (1994) earthquake: effect of structure's number of stories

The characteristics of the earthquake wave at the base of the structure-foundation system affected by *SSI* are divided into inertial and kinematic interactions. Inertial interactions are related to the structure and foundation parameters, while kinematic interactions are related to soil properties. The increase in structure's number of stories produces an extra mass to the structure-foundation system that creates an extra motion at the base compared to *FF* conditions. This motion is manifested by an increase in inertial interaction effects that get more pronounced than kinematic effects, thus dictating the behaviour of the structure. In other words, *SSI* is beneficial to first category structures ($5 \leq N < 10$), while it is detrimental to second category structures ($10 \leq N \leq 15$) founded on silty sandy soil. This is caused by kinematic interaction effects that are greater than inertial interaction effects for the first category, thus dictating the seismic behaviour of the structures to be in parallel with soil behaviour (wave attenuation). The results are in line with those reported by Hayashi and Takahashi (2004) who obtained that structure's damage effect is a function of motion characteristics, structure's number of stories as well as horizontal capacity of the structure's dynamic resistance.

The results presented in Figs. 3 and 4 also show that lateral deflection at the top of the structures increased with storey number provoking shifts in inter-storey drift curves to life threatening and hazardous categories. Note that most seismic codes consider "life safe" as the acceptable limit category. S10, S12 and S15 structures shifted from "life safe" category under El-Centro (1940) earthquake to "near collapse" and "collapse" categories under Northridge (1994) earthquake. Therefore, lateral deflections and thus inter-storey drift results were more affected by the stronger ground motion having higher PGA even though both earthquakes had similar magnitudes. At max top under the influence of El-Centro (1940) earthquake, the ratio of lateral deflection of S15 to S10 flexible cases is equal to 2.33, while the ratio of S15 to S5 flexible cases is equal to 7.87. However, S5 presents higher storey lateral deflection than S15 and S10 at the 5th level for fixed

cases under the influence of El-Centro (1940) earthquake and flexible cases at max abs value under Northridge (1994) earthquake. For example, at max abs value, the ratio of lateral deflection of S15 to S5 is equal to 2.92 and 0.38 under El-Centro (1940) and Northridge (1994) earthquakes, respectively. In addition, as the number of stories increases, the difference in lateral displacement along the different stories between flexible and fixed-based structures increases. This is also caused by the difference in horizontal acceleration between top and base structures. As the number of stories increases, the difference between horizontal acceleration at the top and at the base of the structures tends to decrease for fixed base structures, while for flexible structures, this difference is related to the frequencies obtained from Fourier analyses and to the structure-foundation-soil natural frequencies as will be shown later.

Table 5. Maximum accelerations of the simulated models at base and at top of the structure: effect of number of stories

A_x(m/s^2)	El-Centro (1940)				Northridge (1994)			
Reference name	**Input EQ**	***FF***	**Base**	**Top**	**Input EQ**	***FF***	**Base**	**Top**
S15	3.13	-	3.13	3.46	8.24	-	8.24	8.69
S15-e-1.5m	3.13	0.783	1.33	4.08	8.24	3.13	5.31	6.92
S12	3.13	-	3.13	4.46	8.24	-	8.24	11.22
S12-e-1.2m	3.13	0.78	1.3	3.06	8.24	3.13	5.06	9.19
S10	3.13	-	3.13	4.89	8.24	-	8.24	12.07
S10-e-1m	3.13	0.783	1.32	2.72	8.24	3.13	4.99	10.11
S7	3.13	-	3.13	6.83	8.24	-	8.24	15.19
S7-e-0.7m	3.13	0.783	1.32	3.07	8.24	3.13	5.58	9.97
S5	3.13	-	3.13	8.51	8.24	-	8.24	16.75
S5-e-0.5m	3.13	0.783	1.32	3.4	8.24	3.13	5.77	8.15

Foundation Rocking

The increase in storey number leads to an increase in soil structure interaction effect, thus affecting the amount of flexible structures' distortion and rocking components. These effects, as shown in the previous section, were more pronounced for second category structures. This is in line with Torabi and Rayhani (2014) who found that rigid slender structures were highly affected by *SSI* displayed in their foundation rocking. As detailed in Table 6, foundation rocking angle increased from 0.038° to 0.22° and from 0.11° to 0.44° for S5 to S15 flexible structures under the influence of El-Centro (1940) and Northridge (1994) earthquakes, respectively. To distinguish the contribution of rocking and distortion amount to lateral displacement coming from *SSI* effects, Trifunace et al. (2001 a and b) relationship was used. The relative structure displacement at any level j of the structure is equal to:

$$U_j^{tot} - U_1^{tot} = h_j \emptyset_o + U_j$$

where $U_j^{tot} - U_1^{tot}$ refers to the structural lateral deflection calculated relative to the structure's base, $h_j \emptyset_o$ to the lateral displacement due to rocking component and U_j to lateral displacement due to distortion component. As a result, this relationship calculates the amount of lateral displacement due to rocking and distortion components from the foundation rocking angle. For example, for S10 flexible structures under Northridge (1994) earthquake, foundation rocking

angle was equal to 0.36°. The maximum lateral deflection at the top of S10-e-1m structure equal to 815.69 mm was divided into 193.7 mm as rocking component and 621.96 mm as distortion component, while the lateral deflection of S10 structure was equal to 485.17 mm and was entirely due to distortion component. Subsequently, as the number of stories increased, *SSI* in both structure categories increased foundation rocking angle. Nevertheless, structures with $5 \leq N < 10$ experienced less increase in the amount of rocking component and decrease in the amount of distortion component of flexible structures compared to fixed base structures, as compared to structures with $10 \leq N \leq 15$ reflecting the contribution of inertial and kinematic interaction effects with storey number found in the first section.

Table 6. Maximum foundation rocking (°) of flexible structures: effect of structure's number of stories

Reference name	El-Centro (1940)	Northridge (1994)
S15-e-1.5m	0.22	0.44
S12-e-1.2m	0.16	0.42
S10-e-1m	0.11	0.36
S7-e-0.7m	0.054	0.24
S5-e-0.5m	0.04	0.11

Shear Force and Response Spectrum

Fig. 5 presents the variation of levelling shear forces for the different simulated number of stories cases, while Table 7 illustrates the base shear values and the ratio of base shear of flexible to fixed base cases. As shown in this figure and table and in parallel with the previous sections, structures behaviour is divided into 2 categories: the ratio of flexible to fixed cases base shear was greater than 1 for $10 \leq N \leq 15$ structures, while it was lower than 1 for $5 \leq N < 10$ structures under El-Centro (1940) and close to 1 under Northridge (1994) for all structures. Nevertheless, within the $10 \leq N \leq 15$ category, as the number of stories increased, this ratio decreased. This was caused by *SSI* effects coming from inertial and kinematic effects. As the structure's number of stories increased, inertial effects caused by the mass of the structure-foundation system dominated kinematic effects caused by the ground motion excitations formed in the soil. In fact, structure's base shear tends to increase or decrease depending on the stiffness of the structure and the properties of the soil. This is explained by comparing the accelerations at the base of the structures presented in Table 5 with the base shear values detailed in Table 7. For $5 \leq N < 10$ category, the accelerations at the structures' bases are the same under El-Centro (1940), while they decrease with the increase in number of stories under Northridge (1994). Then, at S10 structure, a shift in overall structural behaviour was obtained reflected by a change in the base shear and acceleration trends. Then, for $10 \leq N \leq 15$ category, the accelerations at the bases slightly increased under El-Centro (1940), while they increased under Northridge (1994) with the increase in structure's number of stories. As for the base shear ratio that tends to decrease within this category, it was caused by the stiffness of the structure that rises with the number of stories.

The simulated results are in parallel with Aviles and Perez-Rocha (1977) who proved that *SSI* effects were larger for tall and slender structures than for short and squat structures of the same period. Moreover, results presented in Fig. 5 indicated that for the same level, the increase in structure's number of stories increased the ratio of flexible to fixed cases shear forces. For example, under El-Centro (1940) earthquake, the ratio of flexible to fixed cases base shear force increased from 0.58 to 1.13, then decreased to 1.00, whereas at the 5th level, the level shear force ratio increased from 0.40 to 0.98 to 1.52 for S5 to S10 to S15. In addition, at the 10th level, it increased from 0.57 to 0.88 for S10 to S15.

Table 7. Base shear ratios of flexible to fixed base cases: effect of structure's number of stories

Reference name	S15-e-1.5m	S12-e-1.2m	S10-e-1m	S7-e-0.7m	S5-e-0.5m
El-Centro (1940)	1	1.1	1.13	0.54	0.58
Northridge (1994)	0.96	0.99	1	1.01	0.97

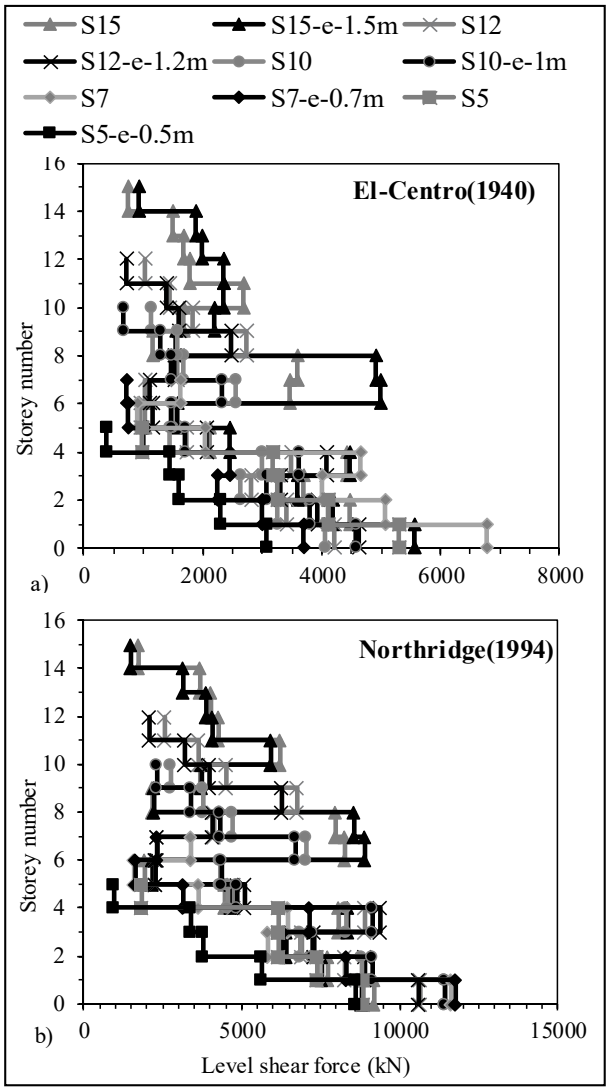

Figure (5): Variation of level shear force with storey number under a) El-Centro (1940) and b) Northridge (1994): effect of structure's number of stories

As the structure's number of stories increases, its natural frequency tends to decrease (Table 8) (Shiming and Gang, 1998). Luco and Wong (1986) and Veletsos et al. (1977) found that *SSI* effects are more significant for high frequencies (short periods) than for low frequencies (long periods) of excitation structures. Therefore, the deviation in the natural frequencies of the structures and soil led to the deviation in *SSI* effects between different structures. As shown in Fig. 6, response spectra amplitude was higher for waves beneath structures compared to *FF* waves even though these waves were not affected by the variation in structure's number of stories by more than 10 %. As detailed in Table 8 and shown in Fig. 7, the first 3 peak frequencies were almost the same for *FF* and structures' base waves under both earthquakes. Nevertheless, comparing these frequencies to the natural frequencies of the simulated models, the results showed that the first- and second-mode natural frequencies of flexible S10 cases were very close to the peak response frequencies obtained from Fourier Analysis. This caused *SSI* effect to be most significant for S10 models, nothing that *SSI* has some unfavourable effect on frequencies between these peak frequencies.

Table 8. Natural frequencies and peak frequencies of the simulated models: effect of structure's number of stories

	Natural frequency (Hz)		Peak frequency of the simulated models (Hz)					
			El-Centro (1940)			Northridge (1994)		
Reference name	***f1***	***f2***	***f1***	***f2***	***f3***	***f1***	***f2***	***f3***
Ground motion	-	-	0.15	0.34	0.49	0.44	0.64	0.88
FF	-	-	0.34	0.59	0.49	0.44	0.64	0.88
S15	0.47	1.45	-	-	-	-	-	-
S15-e-1.5m	0.37	0.5	0.34	0.59	0.83	0.44	0.64	0.88
S10	0.68	2.08	-	-	-	-	-	-
S10-e-1m	0.49	0.55	0.34	0.49	0.59	0.44	0.64	0.88
S5	1.08	3.68	-	-	-	-	-	-
S5-e-0.5m	0.5	0.55	0.34	0.59	0.83	0.44	0.64	0.88

Effect of Raft and Column Dimensions

The effect of raft dimensions of a 15-storey seismic concrete frame structure for two different column sizes (0.5X0.5 m and 0.5X1 m) with 1 m being in the direction of the earthquake load, was investigated in this section.

Sizes were varied between 1.3, 1.5 and 2B (S15-xB) with xB being the width of the structure corresponding to 20 m (1.3B), 22.5 m (1.5B) and 30 m, (2B) with B=15 m, noting that all raft foundations had thicknesses of 1.5 m. Then, raft thicknesses were varied between 1, 1.5 and 2 m (S15-e-y) with e-y being the thickness of the 1.3B (20 m) raft size.

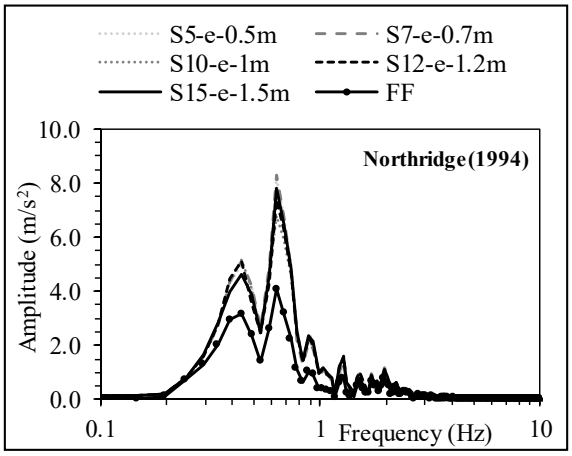

Figure (6): Variation of frequency content with the amplitude under Northridge (1994): effect of structure's number of stories

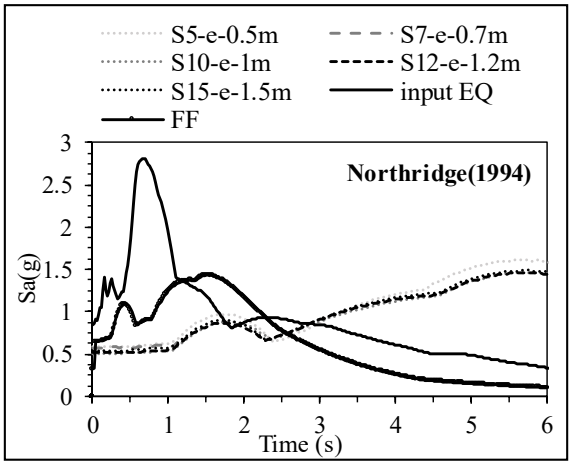

Figure (7): Acceleration response spectrum with 5% damping ratio under Northridge (1994): effect of structure's number of stories

Storey Lateral Deflection and Inter-storey Drifts

Lateral deflection curves presented in Figs. 8 and 9 illustrate the opposite S15 flexible structures' behaviour under the different column sizes while varying raft dimensions. For C 0.5X0.5m, increasing the raft size from 1.3 to 1.5 to 2B amplified the ratio of lateral deflection of flexible to fixed base $\delta_{flexible}/\delta_{fixed}$ S15 structures from 1.9 to 2.61 to 2.66 under El-Centro (1940) and from 1.61 to 1.79 to 1.80 under Northridge (1994). On the other hand, increasing the column size to C 0.5X1m attenuated this ratio from 3.85 to 3.65 to 2.18 under El-Centro (1940) and from 1.64 to 1.62 to 1.58 under Northridge (1994) when increasing the raft size from 1.3 to 1.5 to 2B. Moreover, even though lateral deflections followed the same trend when increasing raft size and thickness, raft thicknesses within the same column size slightly affected lateral deflection and inter-storey drift results. For C 0.5X0.5m, lateral deflection increased 4% and 3%, while for C 0.5X1m, it only decreased by 0.3% and 0.2% from 1 m to 2 m thickness under El-Centro (1940) and Northridge (1994) earthquakes respectively. Furthermore, results indicated that for 1.3B cases (including different raft thicknesses), δ (C 0.5X0.5m) was lower than δ (C 0.5X1m), while for 1.5B and 2B cases, δ (C 0.5X0.5m) was greater than δ (C 0.5X1m).

Like structure's number of stories, increasing the raft and column dimensions increased the structure-foundation system's mass implying a rise in inertial interaction effects. Nevertheless, these effects are related to the structure's base motions coming from kinematic interaction effects. Thus, increasing the column size in the direction of the earthquake load should be beneficial to structures by partially absorbing the earthquake wave. This is illustrated by the decrease in the acceleration of the wave at the base of the structure-foundation system (not shown due to page size limit). The contribution of column size can be clearly detected in fixed cases: even though the wave was amplified under both earthquakes, lateral deflection at top of the fixed-structure decreased from 162.28 mm to 98.77 mm under El-Centro (1940), while it only increased from 643.56 mm to 687.8 mm under Northridge (1994) when increasing column size.

Therefore, for 1.3B cases, the extra mass coming from the columns was not enough for important increase in inertial effects, while for 1.5B and 2B cases, the extra mass coming from both columns and raft sizes led to an important inertial effect rise ending in a reduction in structures' lateral deflections. This reduction was more apparent under El-Centro (1940) earthquake than under Northridge (1994) earthquake. However, the impact on structural safety was more ostensible under Northridge (1994), where structures' performance levels shifted from acceptable "life safe" category to catastrophic "near collapse" and "collapse" categories (not shown due to page size limit). Note that Nguyen et al. (2016), using clayey soil while fixing column size, obtained reduction in lateral deflection curves when increasing raft sizes from 1.1B to 2B for 4 different earthquake loads.

Foundation Rocking

The FE results, presented in Tables 9 and 10, indicate that foundation rocking angle is not only related to the sizes of raft and column, but also to the seismic load. Foundation rocking angle was reduced by the increase in the dimensions of the raft and the decrease in the size of the column. This reduction implies a drop in the rocking component with a rise in the distortion component coming from lateral deflections. This reduction was more under Northridge (1994) earthquake than under El-Centro (1940) earthquake. For illustration, foundation rocking angle increased from 0.44° to 0.78° when increasing column size from C 0.5X0.5m to C 0.5X1m for 1.3B case, while it decreased from 0.44° to 0.17° when increasing raft size from 1.3B to 2B for C 0.5X0.5m under Northridge (1994). Also, for 1.3B cases, increasing the raft thickness from 1 m to 2 m for C 0.5X1m only attenuated rocking angle from 0.24° to 0.23° under El-Centro (1940), while it attenuated it from 0.8 ° to 0.6 ° under Northridge (1994), reflecting the impact of the earthquake characteristics.

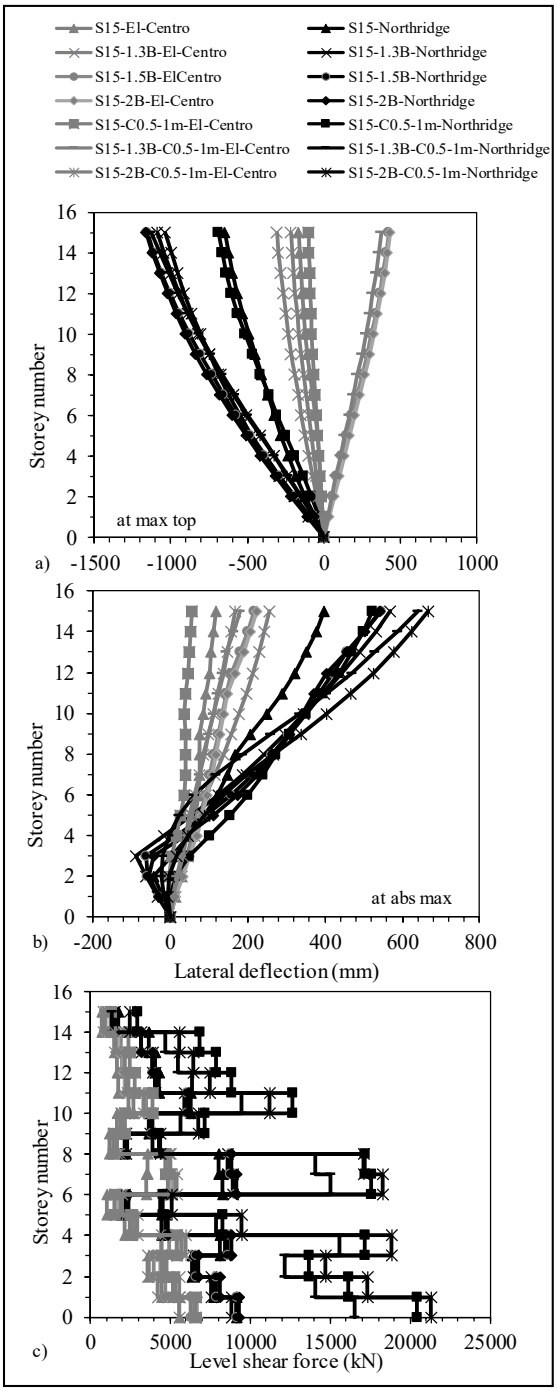

Figure (8): Variation of lateral deflection a) at max top, b) at abs max and c) variation of level shear force with storey number: effect of raft size

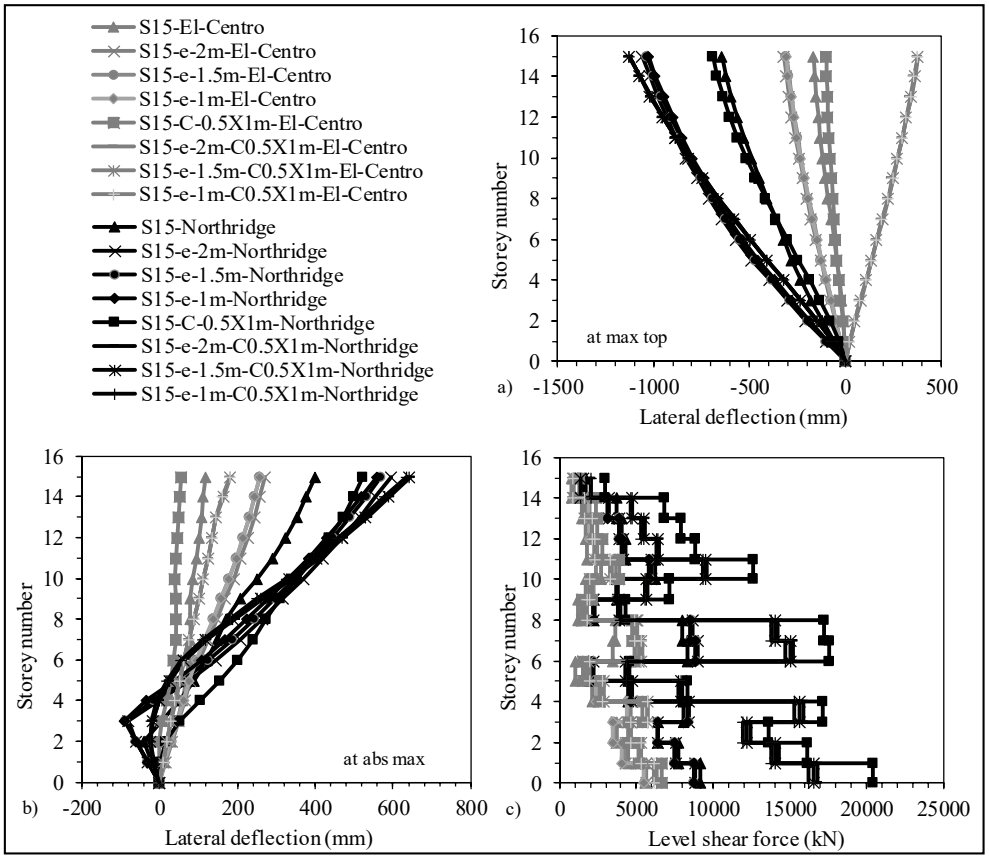

Figure (9): Variation of lateral deflection a) at max top, b) at abs max and c) variation of level shear force with storey number: effect of raft thickness

Table 9. Maximum foundation rocking (°) of flexible structures: effect of raft size

	Reference name	El-Centro (1940)	Northridge (1994)
C-0.5X 0.5m	S15-1.3B	0.22	0.44
	S15-1.5B	0.15	0.31
	S15-2B	0.08	0.17
C-1X 0.5m	S15-1.3B	0.23	0.78
	S15-1.5B	0.13	0.58
	S15-2B	0.07	0.27

Table 10. Maximum foundation rocking (°) of flexible structures: effect of raft thickness

	Reference name	El-Centro (1940)	Northridge (1994)
C-0.5X0.5m	S15-e-1m	0.23	0.45
	S15-e-1.5m	0.22	0.44
	S15-e-2m	0.22	0.43
C-0.5X1m	S15-e-1m	0.24	0.8
	S15-e-1.5m	0.23	0.78
	S15-e-2m	0.23	0.6

Shear Force and Response Spectrum

The results obtained and presented in Tables 11 and 12 as well as in Fig. 8(c) and Fig. 9(c) indicate that base shear ratio of flexible to fixed structures increased with the increase in raft dimensions under both column sizes. It is worth noting that this increase was more apparent between 1.3B and 1.5B cases than between 1.5B and 2B cases. Thus, the contribution of inertial and kinematic effects is reflected not only on lateral deflection results, but also on base shear results. In other words, absorbing part of the wave by the columns was pronounced by a decrease in the wave at the base of the structure-foundation system and an increase in base shear results. For example, under the influence of El-Centro (1940), base shear ratio of 1.3B and 2B increased from 1.0 to 1.2 for C 0.5X0.5m and from 0.95 to 1.01 for C 0.5X1m (Table 11). On the other hand, base shear ratio of 1 m and 2m under El-Centro (1940) increased from 0.98 to 1.02 for C 0.5X0.5m and from 0.93 to 0.96 for C 0.5X1m (Table 12). Regarding response spectrum, results obtained in this paper showed that S_a was slightly affected by the increase in column and raft sizes, like Nguyen (2016) (not shown due to page size limit). This was caused by the ground motion excitations in the soil that depend on the soil properties and earthquake characteristics. 2B to 1.3B C 0.5X0.5m and C 0.5X1m S_a rose only 1.57% and 2.17% and 2.84% and 2.79% under El-Centro (1940) and Northridge (1994) earthquakes, respectively. This is related to peak frequencies obtained from MATLAB (not shown due to page size limit), where peak frequencies of the different simulated models were very close to *FF* condition for both seismic loads. Therefore, *SSI* effect does not only depend on the soil type used (soil properties), but also on the characteristics of the earthquake (magnitude of the earthquake: PGA). As a result, based on overall structural stability and failure, engineers should optimize their designs between column size and raft dimensions. An increase in raft dimensions for the adopted soil properties attracted more shear force and lateral deformation for C 0.5X0.5m, while it attracted more shear force and less lateral deformation for C 0.5X1m. Note that under both column sizes, foundation rocking angle reflected by rocking component was reduced with the increase in raft dimensions.

Table 11. Base shear ratios of flexible to fixed base cases: effect of raft size

	C0.5X0.5m			C0.5X1m		
Reference name	**S15-1.3B**	**S12-1.5B**	**S10-2B**	**S15-1.3B**	**S12-1.5B**	**S10-2B**
El-Centro (1940)	1	1.13	1.20	0.95	1.01	1.01
Northridge (1994)	0.96	1.00	1.02	0.82	0.95	1.04

Table 12. Base shear ratios of flexible to fixed base cases: effect of raft thickness

	C0.5X0.5m			C0.5X1m		
Reference name	**S15-e-1m**	**S15-1.5m**	**S15-e-2m**	**S15-e-1m**	**S15-1.5m**	**S15-e-2m**
El-Centro (1940)	0.98	1.00	1.02	0.93	0.95	0.96
Northridge (1994)	0.95	0.96	0.96	0.79	0.81	0.82

CONCLUSIONS

3D time history nonlinear finite element models of midrise concrete frame structures rested on silty sandy soils were performed using Abaqus under the influence of El-Centro (1940) and Northridge (1994) earthquakes. Flexible and fixed-base structures were simulated and tested for the effects of structure number of stories as well as raft thicknesses and sizes for two different column sizes. Results showed that even though *SSI* provoked an increase in lateral displacement and base shear, it divided midrise structures into 2 categories (1) $5 \leq N < 10$ and (2) $10 \leq N \leq 15$. It was beneficial to the first category and detrimental to the second. This was related to the difference in wave acceleration between the base and top of the structure reflected by the contribution of inertial and kinematic effects. Moreover,

S15 structures behaved differently when increasing raft dimensions (size and thickness) for the different tested column sizes. For 1.3B cases (including tested raft thicknesses), lateral deflection was reduced by the increase in column size, while the opposite behaviour was obtained in 1.5B and 2B cases. Results also showed that base shear was amplified in all cases with the increase in column and raft dimensions, while foundation rocking angle was reduced with the increase in raft dimensions and the decrease in column size. Thus, engineers should optimize column and raft dimensions if they aim at providing overall structural stability, while they should use bigger raft sizes if they want to reduce foundation rocking component.

REFERENCES

Abaqus. [Computer Software]. (2017). "Dassault systems". SIMULIA Corporation, Minneapolis.

Armouni, N.S. (2010). "Effect of dampers on seismic demand of short-period structures." Jordan Journal of Civil Engineering, 4 (4), 367-377.

Armouni, N.S. (2011). "Effect of dampers on seismic demand of short-period structures in rock sites." Jordan Journal of Civil Engineering, 5 (2), 216-228.

AS1170.4. (2007). "Structural design actions-earthquake actions in Australia". Standards Australia, Australia.

ASCE7-10. (2010). "Minimum design loads for buildings and other structures". American Society of Civil Engineers.

ATC. (2002). "Soil-structure interaction for building structures (ATC 84)". Redwood City, California: Applied Technology Council.

Bayat, A., Beiranvand, P., and Ashrafi, H. (2018). "Vibration control of structures by multiple mass dampers." Jordan Journal of Civil Engineering, 12 (3), 461-471.

BSSC. (1997). "NEHRP guidelines for the seismic rehabilitation of buildings". 1997 Edition, Part 1: Provisions and Part 2: Commentary, Federal Emergency Management Agency.

BSSC. (2009). "NEHRP recommended seismic provisions for new buildings and other structures". Federal Emergency Management Agency.

Chopra, A. (2011). "Dynamics of structures theory and applications to earthquake engineering". Prentice Hall, Inc., Fourth Edition.

Djedoui, N., Ounis, A., Mahdi, A., and Zahrai, S. (2018). "Semi-active fuzzy control of tuned mass damper to reduce base-isolated building response under harmonic excitation." Jordan Journal of Civil Engineering, 12 (3), 435-448.

Farghaly, A., and Ahmed, H. (2013) "Contribution of soil-structure interaction to seismic response of buildings." KSCE Journal of Civil Engineering, 17 (5), 959-971.

Fatahi, B., and Tabatabaiefar, S.H. (2014). "Fully non-linear *versus* equivalent linear computation method for seismic analysis of mid-rise buildings on soft soils." International Journal of Geomechanics, 14 (4), 04014016.

Gazetas, G., and Mylonakis, G. (1998). "Seismic soil-structure interaction: new evidence and emerging issues". Proceedings of the Geotechnical Earthquake Engineering and Soil Dynamics III. Reston, Virginia.

Ghosh, S., and Wilson, E.L. (1969). "Dynamic stress analysis of axi-symmetric structures under arbitrary loading". Report no. EERC 69-10, University of California, Berkeley.

Han, Y. (2002). "Seismic response of tall buildings considering soil-pile-structure interaction." Earthquake Engineering and Engineering Vibration, 1 (1), 57-64.

Hayashi, Y., and Takahashi, I. (2004). "Soil-structure interaction effects on building response in recent earthquakes". Proceedings of the 5th International Congress on Computational Mechanics and Simulation ICCMS2014, March 29-30. Chennai, India.

Hokmabadi, A., and Fatahi, B. (2016). "Influence of foundation type on seismic performance of buildings considering soil–structure interaction." International Journal of Structural Stability and Dynamics, 16 (8), 1550043.

Hokmabadi, A., Fatahi, B., and Samali, B. (2012). "Recording inter-storey drifts of structures in time-history approach for seismic design of building frames." Australian Journal of Structural Engineering, 13 (2).

Hokmabadi, A.S., Fatahi, B., and Samali, B. (2014). "Assessment of soil pile-structure interaction influencing seismic response of mid-rise buildings sitting on floating pile foundations." Computers and Geotechnics, 55 (1), 172-186.

Jayalekshmi, B., and Chinmayi, H. (2016). "Effect of soil stiffness on seismic response of reinforced concrete buildings with shear walls." Innovative Infrastructure Solutions, 1 (2).

Kramer, S. (1996). "Geotechnical earthquake engineering". Prentice Hall, Inc.

Kumar, A., Choudhury, D., and Katzenbach, R. (2016). "Effect of earthquake on combined pile-raft foundation." International Journal of Geomechanics, 16 (5), 04016013.

Luco, J.E., and Wong, H.L. (1986). "Response of a rigid foundation to spatially random ground motions." Earthquake Engineering Structural Dynamics, 14 (6), 891-908.

Luco, J.E., Trifunac, M.D., and Wong, H.L. (1988). "Isolation of soil-structure interaction effects by fullscale forced vibration tests." Earthquake Engineering Structural Dynamics, 16 (1), 1-21.

MATLAB and Statistics Toolbox Release. [Computer Software]. (2007b). MathWorks, Inc., Natick, Massachusetts, United States.

Mylonakis, G., and Gazetas, G. (2000). "Seismic soil-structure interaction: beneficial or detrimental?" Journal of Earthquake Engineering, 4 (3), 277-301.

Nadar, J., Chore, H., and Dode, P. (2015). "Soil structure interaction of tall buildings." International Journal of Computer Applications (0975-8887). Published after presenting it at the International Conference on Quality Up-gradation in Engineering, Science and Technology ICQUEST2015, 15-18.

Nguyen, Q., Fatahi, B., and Hokmabadi, A. (2016). "The effects of foundation size on the seismic performance of buildings considering the soil-foundation-structure interaction." Structural Engineering and Mechanics, 58 (6), 1045-1075.

Park, D., and Hashash, Y. (2003). "Soil damping formulation in nonlinear time domain site response analysis." Journal of Earthquake Engineering, 8 (2), 249-274.

Rayhani, M., and El Naggar, M. (2008). "Numerical modeling of seismic response of rigid foundation on soft soil." International Journal of Geomechanics, 8 (6), 15323641.

Seed, H.B., and Idriss, I. (1969). "Influence of soil conditions on ground motion during earthquakes." Journal of Soil Mechanics and Foundation Division, 95 (2), 99-137.

Shatnawi, A., and Al-Qaryouni, Y. (2018). "Evaluating seismic design factors for reinforced concrete frames braced with viscoelastic damper systems." Jordan Journal of Civil Engineering, 12 (2), 202-215.

Shehata, A.E., Ahmed, M., and Alazrak, T. (2015). "Evaluation of soil-foundation-structure interaction effects on seismic response demands of multi-storey MRF buildings on raft foundations." International Journal of Advanced Structural Engineering, 7 (1), 11-30.

Shiming, W., and Gang, G. (1998). "Dynamic soil-structure interaction for high-rise buildings." Developments in Geotechnical Engineering, 83, 203-216.

Stewart, J.P., Fenves, G.L., and Seed, R.B. (1999). "Seismic soil-structure interaction in buildings. I: analytical methods." Journal of Geotechnical and Geoenvironmental Engineering, 125 (1), 26-37.

Tabatabaiefar, S.H., Fatahi, B., and Samali, B. (2014b). "Numerical and experimental investigations on seismic response of building frames under influence of soil-structure interaction." International Journal of Advanced Structural Engineering, 17 (1), 109-110.

Torabi, and Rayhani. (2014). "Three-dimensional finite element modeling of seismic soil–structure interaction in soft soil." Computers and Geotechnics, 60, 9-19.

Trifunac, M., Ivanovic, S.S., and Todorovska, M. (2001a). "Apparent periods of a building. II: time-frequency analysis." Journal of Structural Engineering, 127 (5), 527-357.

Trifunac, M., Todorovska, M., and Hao, T.V. (2001b). "Full-scale experimental studies of soil-structure interaction: a review." Proceedings of the 2nd U.S.-Japan Workshop on Soil-Structure Interaction, March 6-8, Tsukuba City, Japan.

Turan, A., Hinchberger, S.D., and El Naggar, M.H. (2013). "Seismic soil–structure interaction in buildings on stiff clay with embedded basement stories." Canadian Geotechnical Journal, 50 (8).

Veletsos, A., and Meek, J. (1974). "Dynamic behaviour of building foundation system." Earthquake Engineering and Structural Dynamics, 3 (2), 121-138.

Veletsos, A., Prasad, A., and Wu, W.H. (1997). "Transfer functions for rigid rectangular foundations." Earthquake Engineering and Structural Dynamics, 26 (1), 5-17.

Vucetic, M., and Dobry, R. (1991). "Effect of soil plasticity on cyclic response." Journal of Geotechnical Engineering, 117 (1), 89.

Wolf, J.P. (1985). Dynamic soil-structure interaction". Englewood Cliffs, N.J.: Prentice-Hall, Inc.